ISSN 1063-7850, Technical Physics Letters, 2017, Vol. 43, No. 3, pp. 320–323. © Pleiades Publishing, Ltd., 2017.
Original Russian Text © E.E. Timofeeva, E.Yu. Panchenko, Yu.I. Chumlyakov, H.J. Maier, G. Gerstein, 2017, published in Pis'ma v Zhurnal Tekhnicheskoi Fiziki, 2017, Vol. 43, No. 6, pp. 86–94.

Peculiarities of High-Temperature Superelasticity in Ni–Fe–Ga Single Crystals in Compression

E. E. Timofeeva[a], E. Yu. Panchenko[a]*, Yu. I. Chumlyakov[a], H. J. Maier[b], and G. Gerstein[b]

[a] *Tomsk State University, Tomsk, 634050 Russia*

[b] *Institut für Werkstoffkunde, Leibniz Universität Hannover, 30823 Garbsen, Germany*

**e-mail: panchenko@mail.tsu.ru*

Received November 8, 2016

Abstract—The high-temperature superelasticity and temperature dependence of the yield stress of 14M and $L1_0$ martensite in [001]-oriented single crystals of $Ni_{54}Fe_{19}Ga_{27}$ (at %) in compression alloy have been studied. As the temperature increases, the sequence of stress-induced martensitic transformations (MTs) changes from $L2_1$–14M to $L2_1$–$L1_0$. The yield stress of $L1_0$ martensite weakly depends on the temperature and is 1.7 times lower than that of 14M martensite. The temperature interval of superelasticity in [001]-oriented single crystals of $Ni_{54}Fe_{19}Ga_{27}$ under compression is determined by the growth of critical stresses with increasing temperature, the coefficient of strain-hardening, and the yield stress of $L1_0$ martensite.

DOI: 10.1134/S1063785017030245

Intermetallic alloys of the Ni–Fe–Ga system featuring thermoelastic $L2_1$–(10M/14M)–$L1_0$ martensitic transformations (MTs) can find application in high-temperature drives and sensors [1], which stimulates the interest in studying high-temperature MTs in these alloys. High-temperature phenomena of shape memory (SM) and superelasticity (SE) are observed above 373 K, and their manifestations are determined to a considerable degree by mechanical properties of the austenite phase [2]. In [001]-oriented Ni–Fe–Ga single crystals in tension, the SE is observed in the temperature interval from 283 to 700 K as manifested by up to 8% increase in reversible strain [3, 4]. This SE is developed in the entire range of stress-induced MTs up to a temperature of $M_d = 750$ K, where the austenite plastic flow stress is attained [3]. When the deformation mode is changed from tension to compression, [001]-oriented Ni–Fe–Ga single crystals exhibit a strong asymmetry of the interval of SE and the levels of critical stresses for martensite formation and austenite flow [4]. Indeed, the interval of SE does not exceed 180 K (from 283 to 463 K), while the martensite formation stress at $T > 373$ K under compression is twice as large as that under tension [5]. The physical reasons for the SE under compression ending at lower temperatures than under tension are still not completely clear. The temperature dependence of the yield stress of $L2_1$ austenite under compression is insufficiently studied. For establishing a criterion determining the temperature interval of SE in Ni–Fe–Ga single crystals tested at high compressive stresses and high temperatures, it is necessary to study both the temperature dependence of mechanical properties of the high-temperature phase at $T > M_d$ and the temperature dependence of the yield stress of martensite in the entire interval from A_f (reverse MT finish) up to M_d.

The commonly accepted approach to explaining the temperature interval of SE manifestation is based on the comparison of critical stress σ_{cr} of the load-induced MT onset to the yield stress of austenite, $\sigma_{0.1}^{A}$ [2, 6], since the SE usually ends at $\sigma_{cr} \approx \sigma_{0.1}^{A}$. This approach assumes that the mechanical properties of stress-induced martensite are high and this martensite is not subject to dislocation-related plastic flow. If martensite-yield stress $\sigma_{0.1}^{M}$ is close to the critical stress σ_{cr} of the load-induced MT onset, the reverse transition is hindered because of the dislocation pinning of martensite crystals. However, the temperature dependence of the martensite plastic flow stress during intermartensitic transformations in Ni–Fe–Ga single crystals under compression has not been studied so far.

In this context, the present work was aimed at studying the high-temperature SE and temperature dependences of the martensite-yield stress and critical stress for martensite formation in -strained [001]-oriented Ni–Fe–Ga single crystals in compression.

Single crystals of $Ni_{54}Fe_{19}Ga_{27}$ (at %) were grown in an inert gas atmosphere using the Bridgman technique. The as-grown crystals were studied in a single-phase state without additional thermal treatments. As

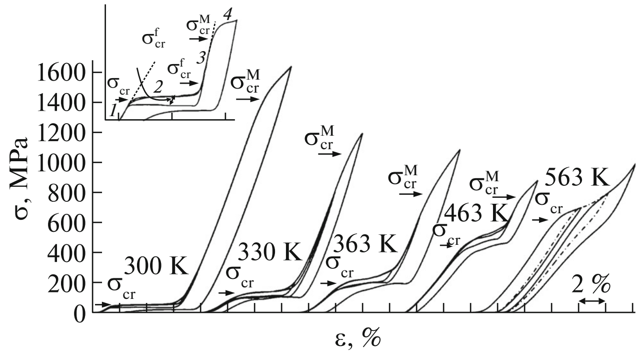

Fig. 1. A series of stress–strain curves σ(ε) measured in the temperature interval of SE. The inset shows a scheme of the SE loop for [001]-oriented Ni–Fe–Ga single crystals in compression (see text for explanations).

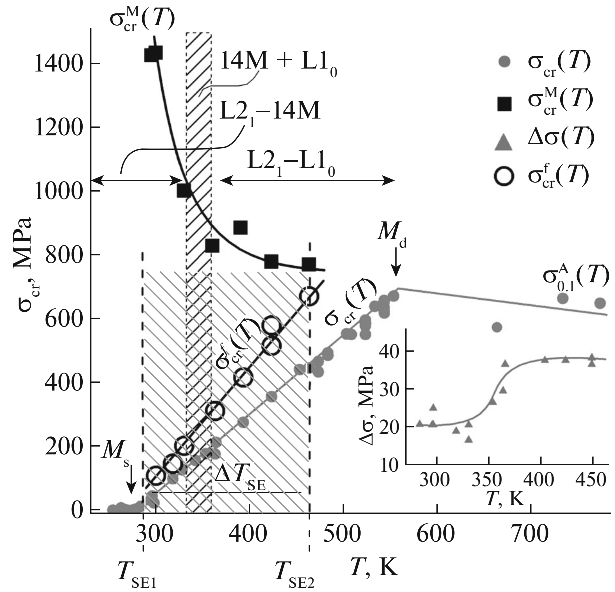

Fig. 2. Temperature dependences of critical stresses for the start (σ_{cr}) and finish (σ^f_{cr}) of the forward MT, martensite-yield stress (σ^M_{cr}), austenite-yield stress ($\sigma^A_{0.1}$), and stress hysteresis Δσ for compression-strained [001]-oriented $Ni_{54}Fe_{19}Ga_{27}$ single crystals in compression.

is known [2–4], the high-temperature phase has an $L2_1$ structure. The samples for testing were shaped as rectangular parallelepipeds with dimensions 3 × 3 × 6 mm. The SM and SE were studied by measuring stress–strain curves σ(ε) during compressive loading and unloading of samples at a constant temperature. The measurements were performed on an Instron 5969 electromechanical testing machine in the temperature interval $T = 295$–623 K and on the setup equipped with a vacuum chamber at temperatures $T > 623$ K. The microstructure of samples was studied by transmission electron microscopy (TEM) on a JEOL 2010 instrument.

Our previous experiments [5] showed that $Ni_{54}Fe_{19}Ga_{27}$ single crystals cooled/heated in the free state exhibit single-stage $L2_1$–14M transformations with the martensite start and finish temperatures $M_s = 273 \pm 2$ K and $M_f = 269 \pm 2$ K, respectively, for the forward MT and the austenite start and finish temperatures $A_s = 279 \pm 2$ K and $A_f = 285 \pm 2$ K, respectively, for the reverse transition. Increase in the temperature of testing is accompanied by variation of the crystalline structure of martensite. In the temperature interval from 283 to 330 K, the loading induces $L2_1$–14M transition as proved by the electron-microscopic data [5]. Increase in the temperature up to 360 K leads to a change in the MT order, so that $L2_1$–$L1_0$ transition is observed under loading in the T = 360–463 K interval.

Figure 1 shows a series of stress–strain curves σ(ε) measured during compressive loading/unloading under isothermal conditions. These curves were used to determine the values of critical stress σ_{cr} for stress-induced martensite formation, which are plotted in Fig. 2. The observed increase in σ_{cr} with temperature has a linear character in agreement with the Clausius–Clapeyron equation [2]:

$$\frac{d\sigma_{cr}}{dT} = -\frac{\Delta S}{\varepsilon_{tr}} = -\frac{\Delta H}{\varepsilon_{tr}T_0}, \qquad (1)$$

where ΔS is a change in the entropy, ΔH is a change in the enthalpy upon transformation per unit volume, ε_{tr} is the transformation strain, and T_0 is the temperature of chemical-phase equilibrium.

Previously, it has been established [2] that tensile straining of [001]-oriented Ni–Fe–Ga single crystals as also accompanied by a change in the sequence of MTs from $L2_1$–14M–$L1_0$ to $L2_1$–$L1_0$, which is manifested by the appearance of two stages in the $\sigma_{cr}(T)$ curve with high ($\alpha_1 = d\sigma_{cr}/dT = 1.7$ MPa/K) and low ($\alpha_2 = d\sigma_{cr}/dT = 0.5$ MPa/K) slopes characterizing the temperature-induced growth of stresses. According to Eq. (1), the value of $\alpha = d\sigma_{cr}/dT$ is inversely proportional to the transformation strain ε_{tr}. The two stages in tensile-strained crystals appear because the ε_{tr} value (6.4% for $L2_1$–14M) at the first stage is smaller than that (13.5% for $L2_1$–$L1_0$) at the second stage). In the case of compression, a change in the order of MTs under load does not influence the slope α = 2.1 MPa/K, since the ε_{tr} value for 14M and $L1_0$ structures is the same.

A change in the MT sequence in Ni–Fe–Ga single crystals in compression can be revealed by studying the temperature dependence of stress hysteresis Δσ(T) (Fig. 2). During the formation of 14M martensite in the interval from 283 to 330 K, the hysteresis weakly depends on the temperature and amounts to Δσ ≈ 20 ± 1 MPa. At T = 360–463 K, the load-induced $L2_1$–$L1_0$ transition is accompanied by a wider hysteresis

($\Delta\sigma \approx 40 \pm 1$ MPa) as compared to that for $L2_1$–14M, but also weakly dependent on the temperature. Under the action of compressive loading in [001] direction, no twinning of 14M and $L1_0$ martensite was observed [4, 7, 8]. Therefore, the MT is not accompanied by distortion and/or rotation of the habit plane relative to the invariant position, which usually leads to increased energy scattering. Thus, the increase in MT stresses with the temperature influences neither the twinned martensite structure nor the stress hysteresis width, which explains the weak temperature dependence of $\Delta\sigma(t)$ at $T < 330$ K and $T > 360$ K. In the interval of 330–360 K, the increase in hysteresis is related to a change in the martensite structure to $L1_0$. Indeed, it was shown [7, 9] that an undistorted habit plane is formed more readily between $L2_1$ and 14M structures than between $L2_1$ and $L1_0$, since 14M martensite contains a high density of microtwins and represents an ordered modulated structure.

As can be seen from Fig. 1, $\sigma(\varepsilon)$ curves of samples in compression reveal four stages related to (*1*) elastic deformation of austenite, (*2*) stress-induced MT, (*3*) elastic deformation of martensite, and (*4*) plastic deformation of martensite. Increasing temperature leads to growth in critical stress σ_{cr} for the onset of stress-induced MT, increase in stage *1*, decrease in reversible transformation strain at stage *2*, and decrease in the martensite-yield stress at stage *4*. A strong decrease in the reversible strain (from 6.2% at 273 K to 2.9% at 463 K) is not related to modification of the martensite structure, since the theoretical values of the transformation strain upon the formation of $L1_0$ and 14M structures are the same (6.25%) [4, 7]. A decrease in the level of strain can be explained as follows. As can be seen from the $\sigma(\varepsilon)$ curves, the effective elastic modulus of austenite (E_A) is much lower than that of martensite (E_M). The low modulus of austenite indicates that its lattice prior to the start of stress-induced MT is subject to significant elastic distortions and the lattice parameter changes so as to approach the lattice parameter of martensite.

It was shown for TiNi [10] and NiFeGaCo [11] alloys that reversible strain ε_{rev} can be related not only to the transformation of austenite to martensite, but also to the difference of effective elastic moduli E_A and E_M:

$$\varepsilon_{rev} = \varepsilon_{tr} + \left[\frac{1}{E_M} - \frac{1}{E_A}\right]|\sigma_{cr}|, \qquad (2)$$

where σ_{cr} is the critical stress. In [001]-oriented Ni–Fe–Ga single crystals under compression, $E_A < E_M$ (Fig. 1) and, hence, the second term in relation (2) is negative. Since the level of critical stresses σ_{cr} increases with the temperature, the second term also grows while the reversible strain decreases.

Figure 2 presents the results of investigation of the temperature dependences of martensite-yield stress ($\sigma_{0.1}^{M}$) and critical stresses for the start (σ_{cr}) and finish (σ_{cr}^{f}) of the forward MT. The martensite with 14M structure contains a high density of twins, which hinder the development of dislocation glide. For this reason, the yield stress upon 14M martensite formation is high and amounts to $\sigma_{0.1}^{M}[001] = 1430$ MPa. As the structure of stress-induced martensite changes from 14M to $L1_0$, the yield stress sharply drops to 830 MPa at 360 K. For $T > 360$ K, the final structure upon MT becomes $L1_0$ and the yield stress weakly decreases to 775 ± 2 MPa as the temperature grows further to 463 K. At the same time, the value of σ_{cr}–σ_{cr}^{f} for the forward MT increases with the temperature and, accordingly, the strain-hardening coefficient $\theta = d\sigma/d\varepsilon$ grows from 2×10^2 MPa at 295 K up to 21×10^2 MPa at 463 K. The growth of critical stress σ_{cr} for the load-induced MT onset and the strong increase in coefficient $\theta = d\sigma/d\varepsilon$ result in that the critical stress for the forward MT finish at 463 K ($\sigma_{cr}^{f} = 700$ MPa) becomes close to the martensite-yield stress $\sigma_{0.1}^{M} = 775 \pm 2$ MPa (Fig. 2). Thus, the MT at temperature $T_{SE2} = 463$ K corresponds to the last perfect SE loop, for which the entire preset strain in the loading/unloading cycle upon the MT completion is reversible.

At temperatures within 463 K $< T <$ 543 K, [001]-oriented Ni–Fe–Ga single crystals in compression also feature the thermoelastic $L2_1$–$L1_0$ transitions, the critical stresses of which increase with the temperature with same slope ($\alpha = d\sigma_{cr}/dT = 2.1$ MPa/K) as that for $T < T_{SE2}$. In this temperature interval, $\sigma_{cr}^{f} > \sigma_{0.1}^{M}$ and the MT is accompanied by microplastic deformation and stabilization of $L1_0$ martensite, while the preset strain remains partly irreversible upon unloading. Electron-microscopic images of samples in compression in this interval reveal residual $L1_0$ martensite and high density of dislocations (Fig. 3). When the temperature approaches $M_d \sim 550$ K, the entire preset strain become irreversible upon unloading (see Fig. 1, curve for $T = 543$ K). It can be suggested that the sample in compression at $T \sim 550$ K simultaneously features the MT and the plastic deformation of austenite and martensite. It should be noted the cyclic loading at 543 K leads to dislocation-induced hardening of the alloy. As can be seen from Fig. 1, a preliminary deformation at 543 K leads to the partial recovery of reversibility (see the third $\sigma(\varepsilon)$ curve for $T = 543$ K).

Thus, the temperature interval $\Delta T_{SE} = T_{SE2}$–T_{SE1} of SE in [001]-oriented Ni–Fe–Ga single crystals in compression is determined by the values of slope $d\sigma_{cr}/dT$ (characterizing growth of the critical stresses of martensite formation with the temperature), strain-hardening coefficient $\theta = d\sigma/d\varepsilon$, and mechanical properties of the austenite and martensite phases. This

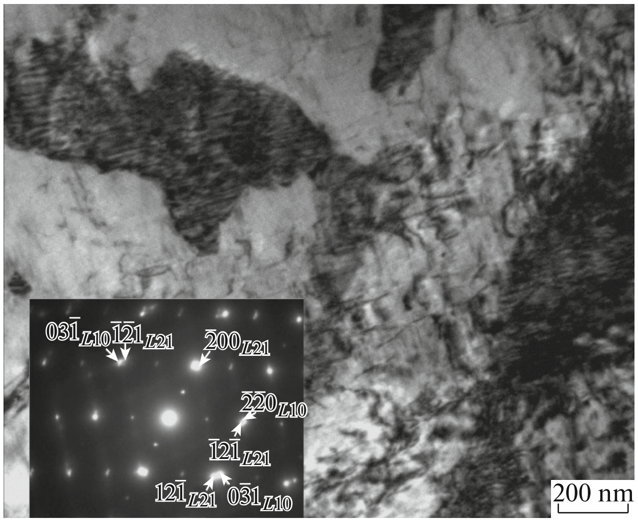

Fig. 3. Bright-field electron-microscopic image of [001]-oriented Ni–Fe–Ga single crystal after compression loading at $T > T_{SE2}$. The inset shows the corresponding pattern of electron microdiffraction (axis of zone $[1\bar{1}3]_{L10} \parallel [012]_{L21}$).

complex criterion represents a modification (improvement) of the criterion proposed previously for some SM alloys [2]. The new variant can be used for description of the interval of SE in other SM single crystals, including [001]-oriented Ni–Fe–Ga single crystals in compression. The high-temperature SE in a broad temperature range in the latter crystals requires only high strength of austenite and low values of $\alpha = d\sigma_{cr}/dT$, since the level of plastic flow stress $\sigma_{0.1}^{M}$ in martensite is not attained during the stress-induced MT, while the train hardening coefficient $\theta = d\sigma/d\varepsilon$ is close to zero in the entire temperature range of SE.

Acknowledgments. This study was supported in part by the Russian Foundation for Basic Research (project no. 14-08-00946) and the Presidential Program of Support for Young Russian Scientists (project no. MK-8884.2016.8).

REFERENCES

1. V. I. Nikolaev, P. N. Yakushev, G. A. Malygin, A. I. Averkin, S. A. Pulnev, G. P. Zograf, S. B. Kustov, and Yu. I. Chumlyakov, Tech. Phys. Lett. **42**, 399 (2016).
2. Yu. I. Chumlyakov, I. V. Kireeva, E. Yu. Panchenko, E. E. Timofeeva, Z. V. Pobedennaya, S. V. Chusov, I. Karaman, H. Maier, E. Cesari, and V. A. Kirillov, Russ. Phys. J. **51**, 1016 (2008).
3. Yu. Chumlyakov, I. Kireeva, E. Panchenko, et al., J. Alloys Compd. **577**, S393 (2013).
4. R. F. Hamilton, H. Sehitoglu, C. Efstathiou, and H. J. Maier, Acta Mater. **55**, 4867 (2007).
5. E. E. Timofeeva, E. Yu. Panchenko, Yu. I. Chumlyakov, and A. I. Tagil'tsev, Vestn. Tambov. Univ. **18**, 1617 (2013).
6. Y. Liu and S. P. Galvin, Acta Mater. **45**, 4431 (1997).
7. Y. Sutou, N. Kamiya, T. Omori, et al., Appl. Phys. Lett. **84**, 1275 (2004).
8. S. Kaufmann, U. K. Roßler, O. Heczko, et al., Phys. Rev. Lett. **104**, 145702 (2010).
9. C. Efstathiou, H. Sehitoglu, J. Carroll, et al., Acta Mater. **56**, 3791 (2008).
10. Y. Liu and H. Yang, Mater. Sci. Eng. A **260**, 240 (1999).
11. E. Panchenko, Y. Chumlyakov, H. J. Maier, et al., Intermetallics **18**, 2458 (2010).

Translated by P. Pozdeev